

MPD

ARIADNA

BM@N

SPD

Applied research with heavy ion beams

Issues of Life Sciences, Materials Sciences and related fields

Oleg Belov

Veksler and Baldin Laboratory of High Energy Physics
Joint Institute for Nuclear Research
E-mail: oleg.belov@jinr.int

Outline

I. Basics of interaction of heavy ions with matter

II. Applied research with NICA heavy ion beams

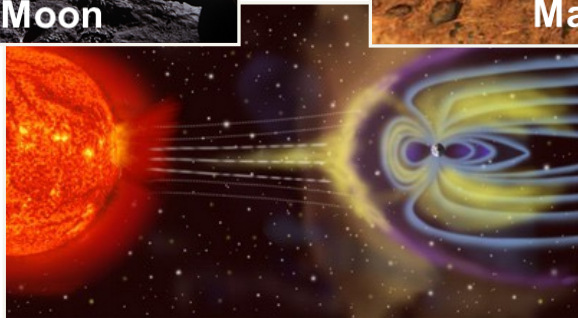
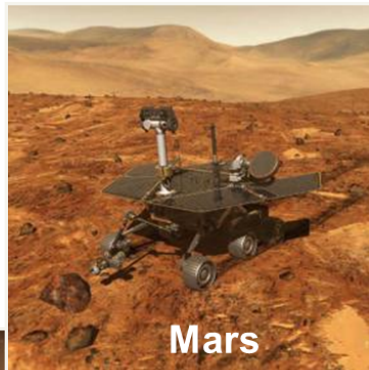
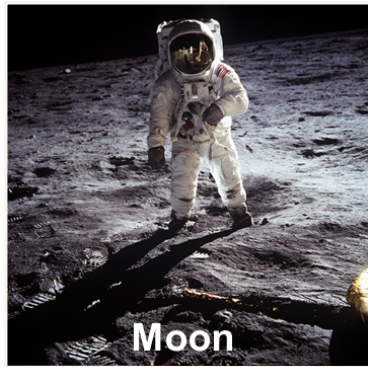
III. Sample activities and selected results

IV. Ways to be involved in the ARIADNA collaboration
on applied research at NICA

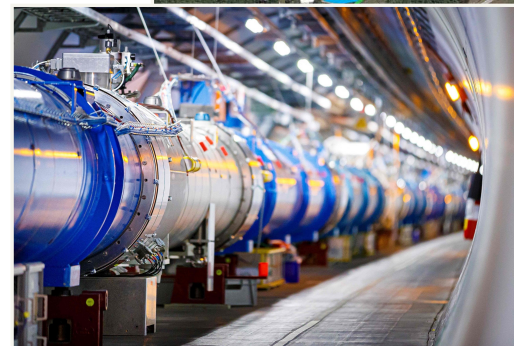
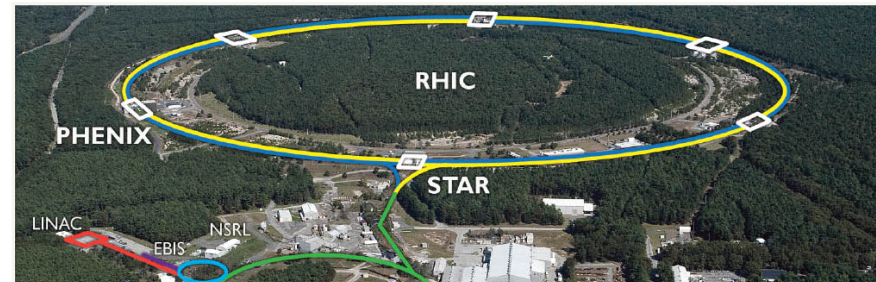
Natural and artificial sources of heavy ions



Space radiation



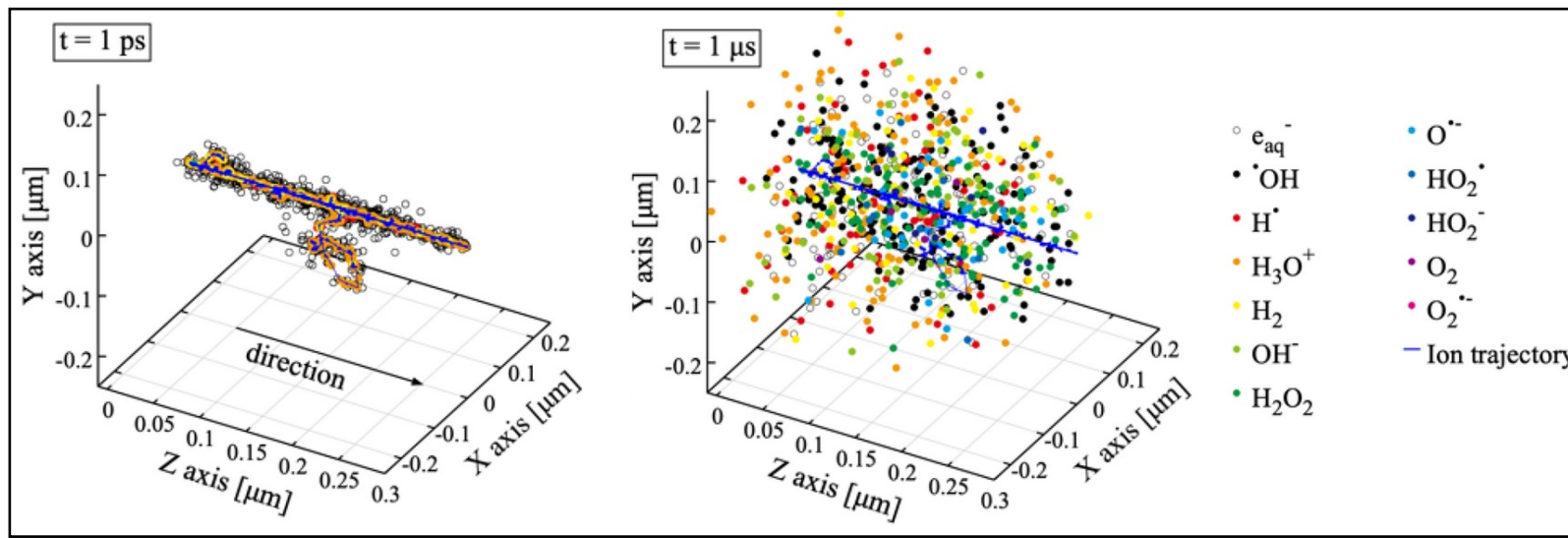
Particle accelerators



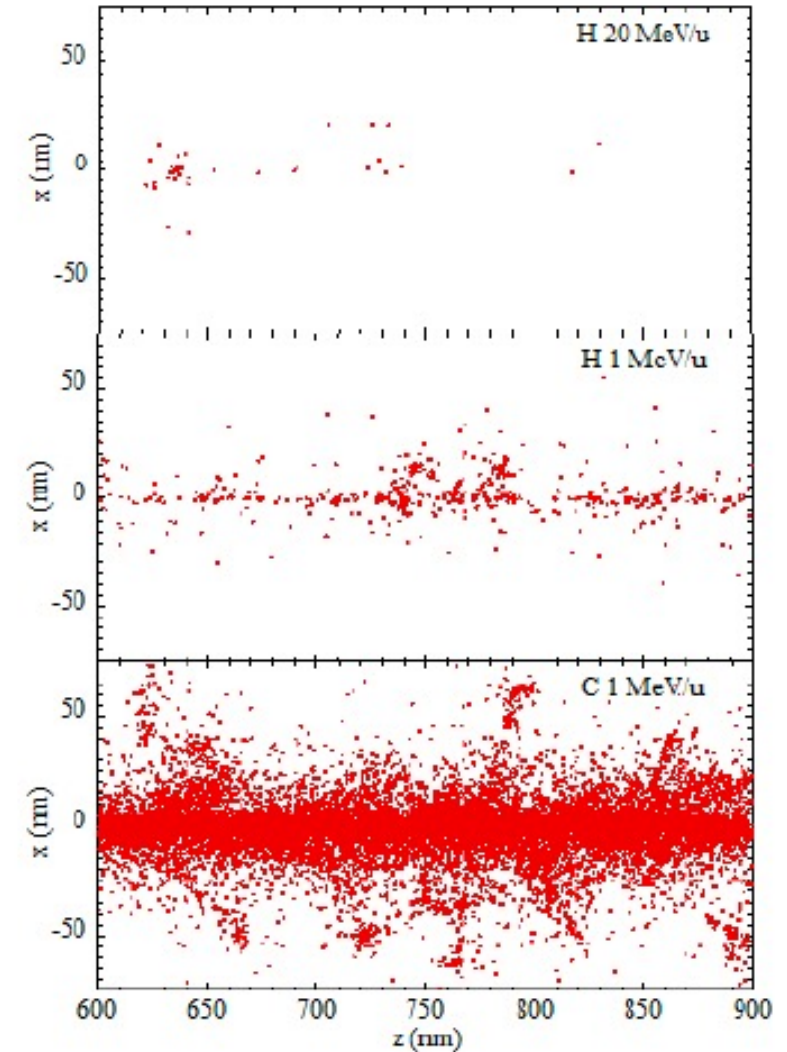
HEAVY IONS: INTERACTION WITH MATTER

In many solids heavy ions release sufficient energy to induce permanently modified cylindrical zones, so-called **ion tracks**.

In biological matter heavy ions leave a trace of damage to biomolecules and induce a cascade of water and organic **radiolytic specie production**, which evolves with time.

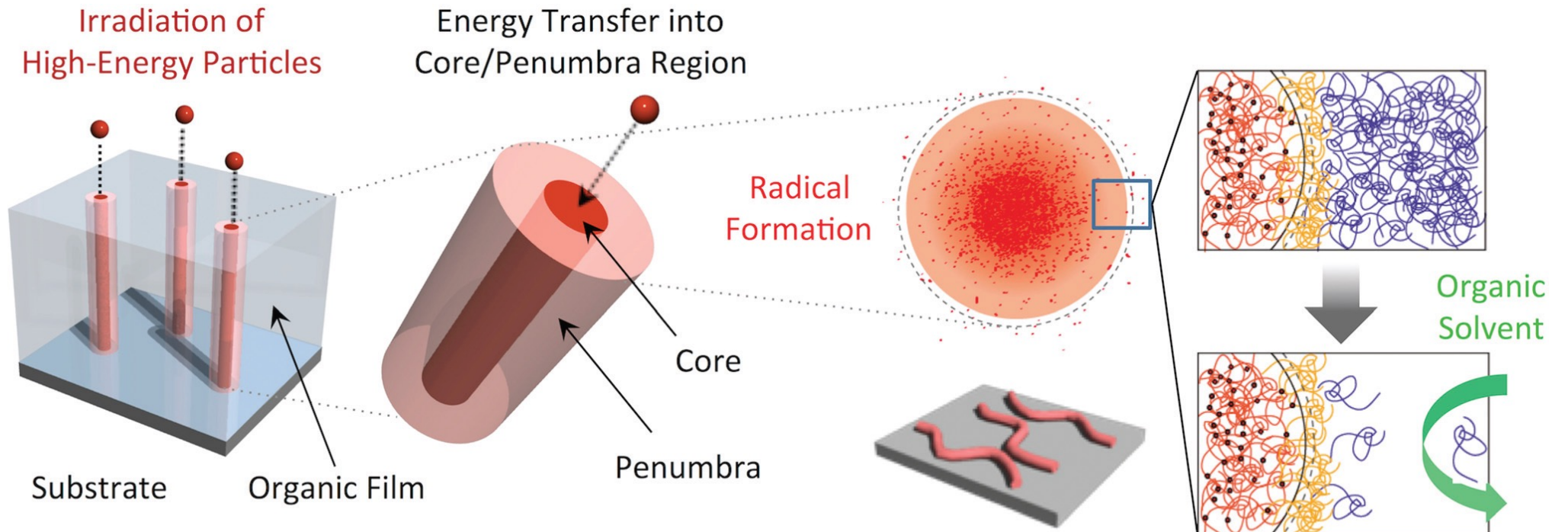
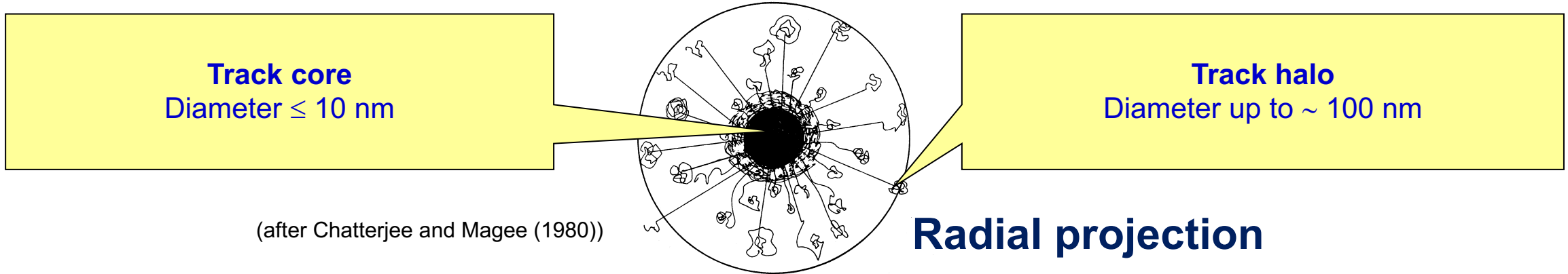


Chemical evolution of 400 MeV/u carbon ion track in water in the time 1 ps to 1 μs (Baba, K., Kusumoto, T., Okada, S. *et al. Sci Rep* 11, 1524, 2021)



Y. Ngon-Ravache, M. Ferry, S. Esnouf, E. Balanzat. 2nd Int. Workshop Irradiation of Nuclear Materials: Flux and Dose Effects (2016)

STRUCTURE OF AN ION TRACK



DOSIMETRY WITH HEAVY ION BEAMS: BASICS AND MAIN PROBLEMS

The conventional dosimetry operates mainly with macroscopic quantity being the **absorbed dose**.

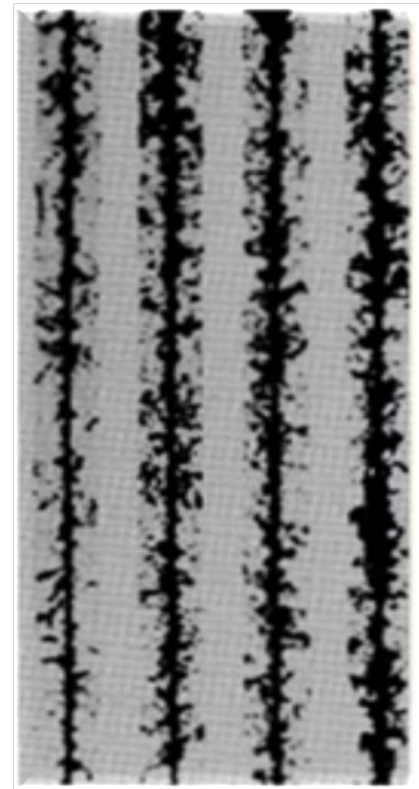
The absorbed dose, D , is the quotient of $d\bar{\epsilon}$ by dm , where $d\bar{\epsilon}$ is the mean energy imparted by ionizing radiation to matter of mass dm , thus

$$D = \frac{d\bar{\epsilon}}{dm} \quad \text{/ICRU Report No. 85/}$$

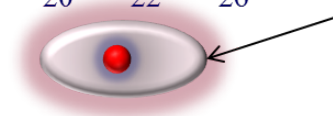
Unit: J kg^{-1}

The special name for the unit of absorbed dose is gray (Gy).

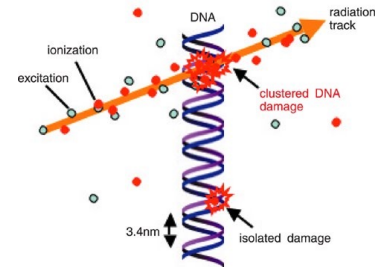
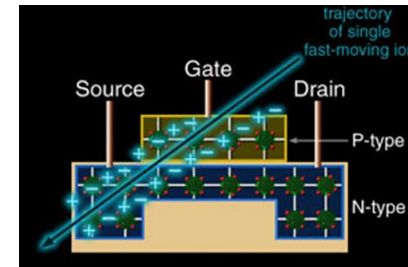
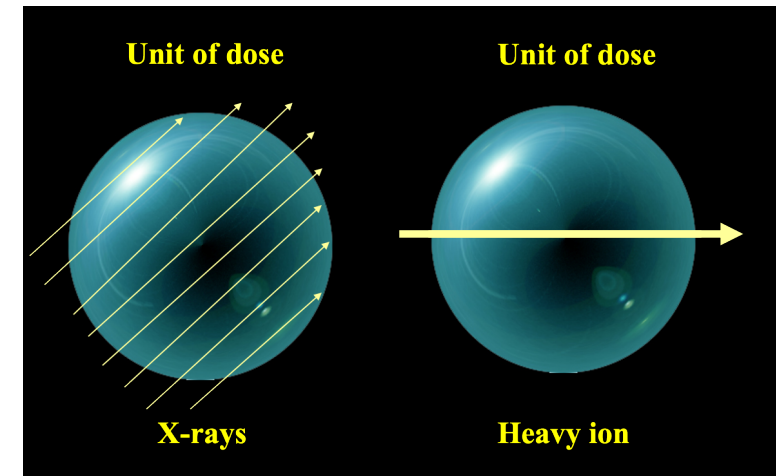
The macroscopic dosimetry with heavy ions works nice in the case of solids but falls with small objects (biomolecules, living cells, microelectronic devices, etc.).



Si Ca Ti Fe
Z = 14 20 22 26



Mammalian cell



From their very beginning, experiments with heavy ions and small targets like living cells and biomolecules have identified the problem of microdosimetry because of their stochastic nature of energy deposition.

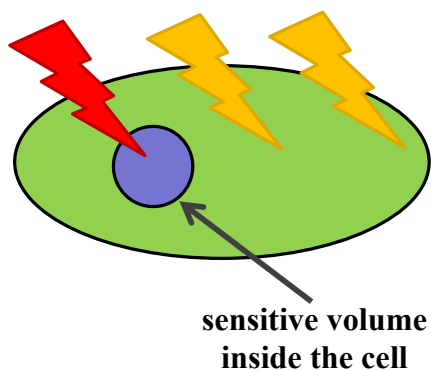
FROM CONVENTIONAL DOSIMETRY TO MICRODOSIMETRY

The early **target theories** attempted to describe the discrete acts of energy transfer, termed “**hits**” identifying them with individual ionizations or clusters of ions.

The spatial correlation of these events was not considered, and target theory in this earliest form could not explain the relative biological effectiveness of different types of ionizing radiation.

Three principles of the target theory:

1. The cell has an unique target smaller than the cell and sensitive to radiation.
2. Radiation energy is transferred to the cell in a discrete way.
3. Separate acts of energy deposition occur independently.



$$\bar{n} = VD$$



$$P_{(k)} = \frac{e^{-\bar{n}} \bar{n}^k}{k!}$$

Poisson distribution

$$P_{(0)} = e^{-VD}$$

Probability of cell survival

• Classical models



• Stochastic models



• Probabilistic models



• Repair models



• Molecular models

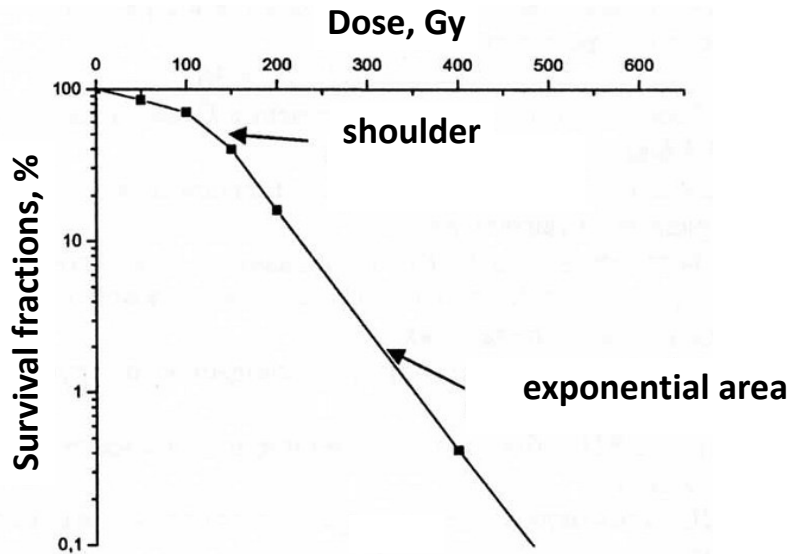


• Models taking into account the radiation quality

Later on, it was shown that the **V** parameter depends on many physical and biological factors. This fact did not allow to interpret correctly the exponential survival curves.

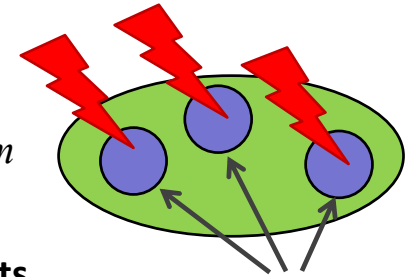
EVOLUTION OF CLASSICAL MODELS FOR CELL SURVIVAL

One more problem: the analysis of survival curves having a “**shoulder**”



Multi-target formula: $P'_{(m)} = 1 - (1 - e^{-VD})^m$

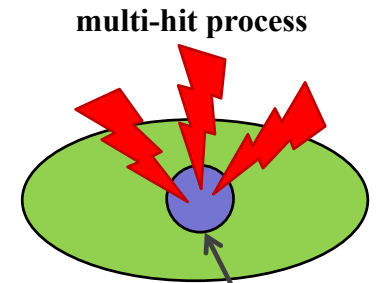
where m is the number of targets



several sensitive volumes inside the cell

Multi-hit formula: $P'_{(n)} = e^{-VD} \sum_{k=0}^{n-1} \frac{(VD)^k}{k!}$

where n is the number of hits



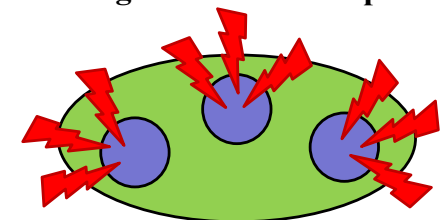
multi-hit process

sensitive volume inside the cell

Multi-target and multi-hit formula: $P'_{(n,m)} = 1 - \left(1 - e^{-VD} \sum_{k=0}^{n-1} \frac{(VD)^k}{k!} \right)^m$

m is the number of targets, n is the number of hits

multi-target and multi-hit process



- The parameters m and n do not have a real biophysical meaning.
- These parameters vary significantly under changes of some physical and biological factors.

STOCHASTIC MODELS

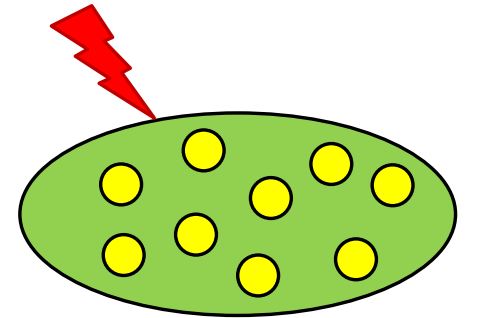
Cells irradiated with the same dose have an equal probability of successful division (of survival). But as the cell division process is stochastic (depending on biological variability), cell survival is probabilistic.

Suggesting the equal number of initial lesions in cells, it is supposed that each lesion is caused by changes in the number of some cell structures. These changes lead to an increase in the **failure probability** during cell division.

$$-dN = S' N_0 dt$$

dN is the number of surviving cells;
 N_0 is the initial number of cells;
 $S'(t, D)$ is the failure probability during cell division in the t unit of time.

If the failure probability increases linearly with the irradiation dose $S'(t, D) = S'_1(t)D$



Then an exponential curve can be obtained:

$$N = N_0 e^{-D \int_0^{\infty} S'_1(t) dt}$$

To take into account the **target theory**, a vector is introduced, which characterizes a cell population: $\xi = (\xi_1, \xi_2, \dots, \xi_n)$.

The initial state corresponds to $\xi_0 = (1, 0, \dots, 0)$. Under the irradiation of the cell population ξ with the dose dD , this population transforms into a new state $\xi + d\xi = \xi + A\xi dD$, where A is a matrix of transition probabilities of the $n \times n$ order. The solution of this equation is $\xi = \xi_0 e^{AD}$.

If we suppose that cells in state $n - 1$ are able to repair the damage and in the state n they die, then the survival curve can be described as

$$S = \sum_{k=1}^{n-1} \xi_k$$

The main problem with the stochastic models is the assumption on the same vulnerability of cells exposed to same dose.

PROBABILISTIC MODELS

Probabilistic models combine the **target theory** and **biological stochasticity**.

Let us put $\alpha < 1$ which is the probability of a failure in cell division (the probability of cell death), and $P_1 = 1 - \alpha$ is the probability of successful cell division (survival). Then, this probability for cells with i lesions will be

$$P_i = (1 - \alpha)^i$$

(based on the assumption that all lesions are independent on each other).

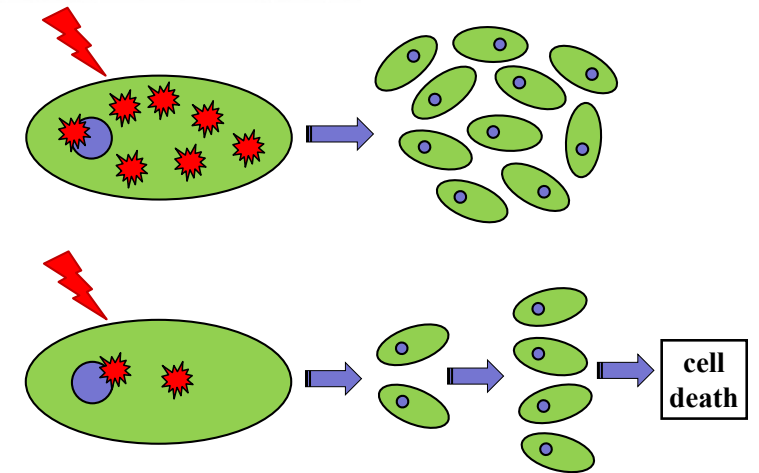
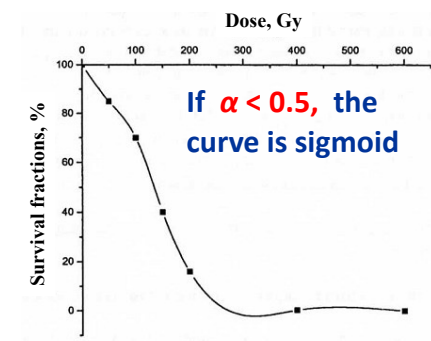
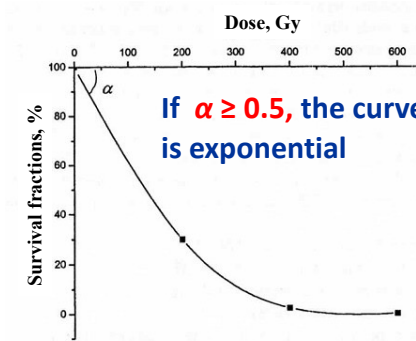
Cell survival is described as
$$S = \sum_{i=0}^k \frac{e^{-a} a^i}{i!} \left(1 - \left(\frac{1 - (1 - \alpha)^i}{(1 - \alpha)^i} \right)^2 \right)$$

Here b is the probability of lesion formation per unit dose;

$a = bD$ is the average number of lesions;

k is the number of lesions when $(1 - \alpha)^k > 0.5 \geq (1 - \alpha)^{k+1}$.

The curves calculated using probabilistic models are superpositions of several multi-hit curves with the critical number of hits from **0** to **k**.



Probabilistic models can reconstruct different types of survival curves and explain some effects of irradiation. **But** they do not take into account the possibility of **damage repair**, which determines the different **outcomes**.

REPAIR MODELS

The cell inactivation caused by radiation is connected with the **repair process**.

$$S = e^{-kD + \alpha(1 - e^{-\beta D})}$$

kD is the number of cell lesions (proportional to the dose D);

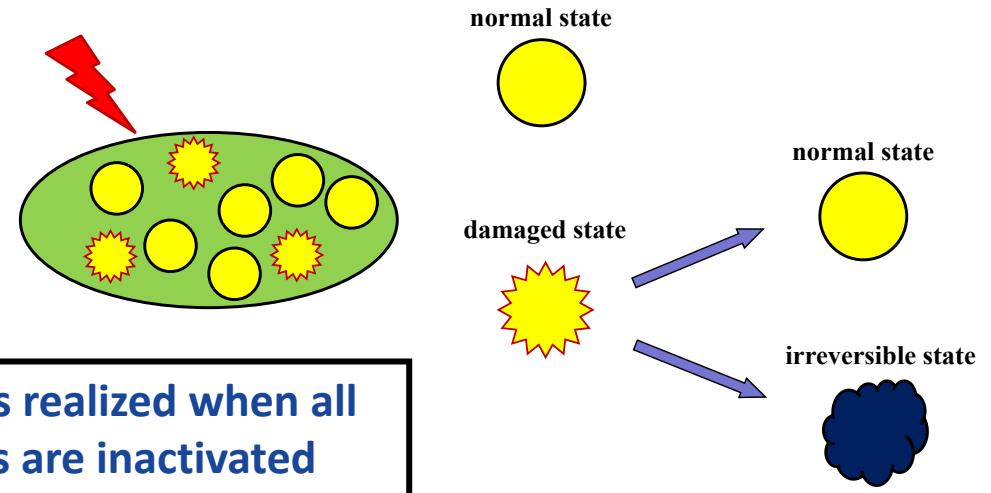
$\alpha(1 - e^{-\beta D})$ is the number of repaired lesions;

α is the probability of a failure in cell division (probability of cell death);

β is the probability of damage repair per unit dose.

The repair models described the induction and elimination of lesions only formally and **did not take into account real intracellular biophysical mechanisms**.

Each target can be in two states



Cell death is realized when all such targets are inactivated

MOLECULAR MODELS

Molecular models assumes a dependence of the cell survival on the **position of radiation-induced damage at the DNA molecule.**

The lethal outcome for the cell is the induction of a straight double-strand DNA break or two overlapping single-strand DNA breaks.

$$S = e^{-\alpha D - \beta D^2}$$

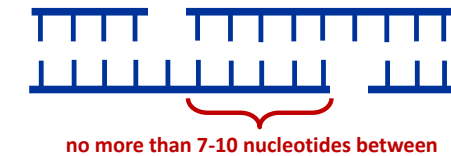
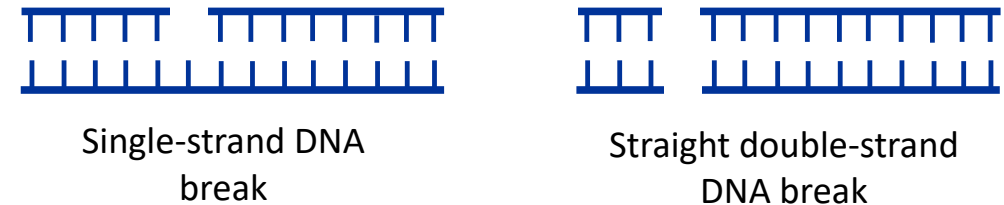
α is the probability of the induction of a straight double-strand break;

β is the probability of the induction of a double-strand break from two overlapping single-strand breaks.

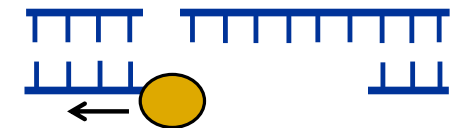
$$S = e^{-N\beta D} \left(1 - e^{-\frac{l_0 \beta D}{M}} \right)$$

β is the yield of the initial DNA lesions; l_0 is the size of a DNA gap; M is the genome size; N is the factor of the nearest non-simultaneous lesions in the opposite DNA strands.

Such curves have a small shoulder in the low-dose region and an exponential part at the high levels of irradiation.



Double-strand break produced by the overlapping of two single-strand ones

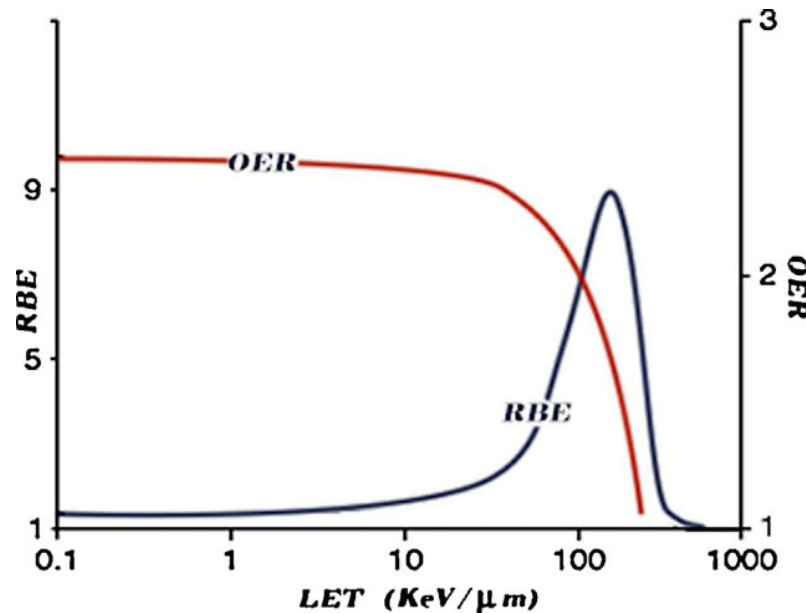
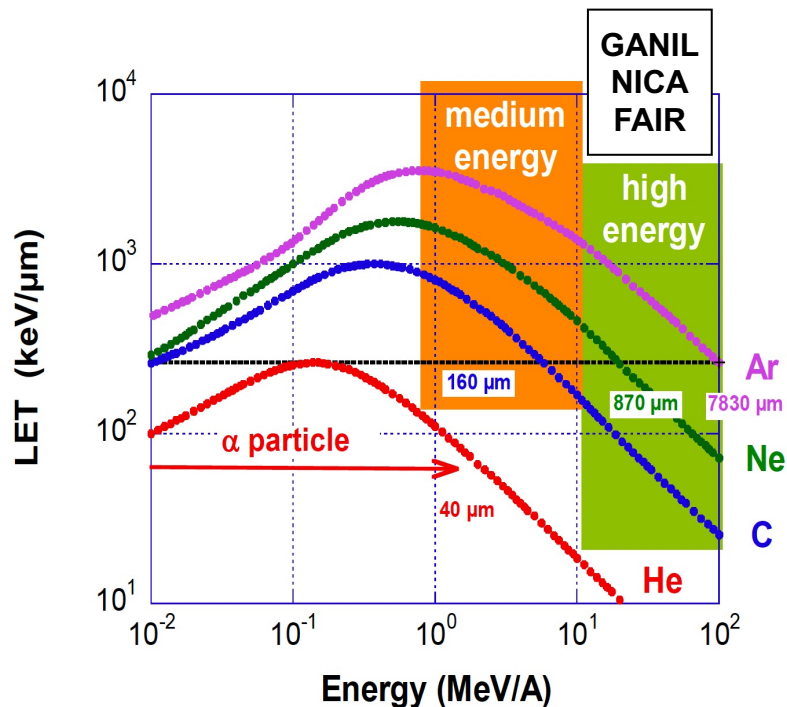


Double-strand break produced by the enzymatic degradation of DNA

MODELS TAKING INTO ACCOUNT THE RADIATION QUALITY

More realistic models were proposed through a more detailed description of the “random” configurations of energy deposition in the tracks of charged particles.

The term “Linear Energy Transfer” or LET was introduced to characterize how a particle loses energy along its track. The LET basically determines the radiation quality.



Linear energy transfer

$$L = \frac{dE}{dx}$$

The energy dE lost per unit length dx of particle track in the matter.

Unit: keV/μm

In **microdosimetry** one is interested in measuring or estimating the **distribution of energy transfer along a particle's track**.

Therefore the quantities used in microdosimetry are somewhat different than those used in conventional dosimetry.

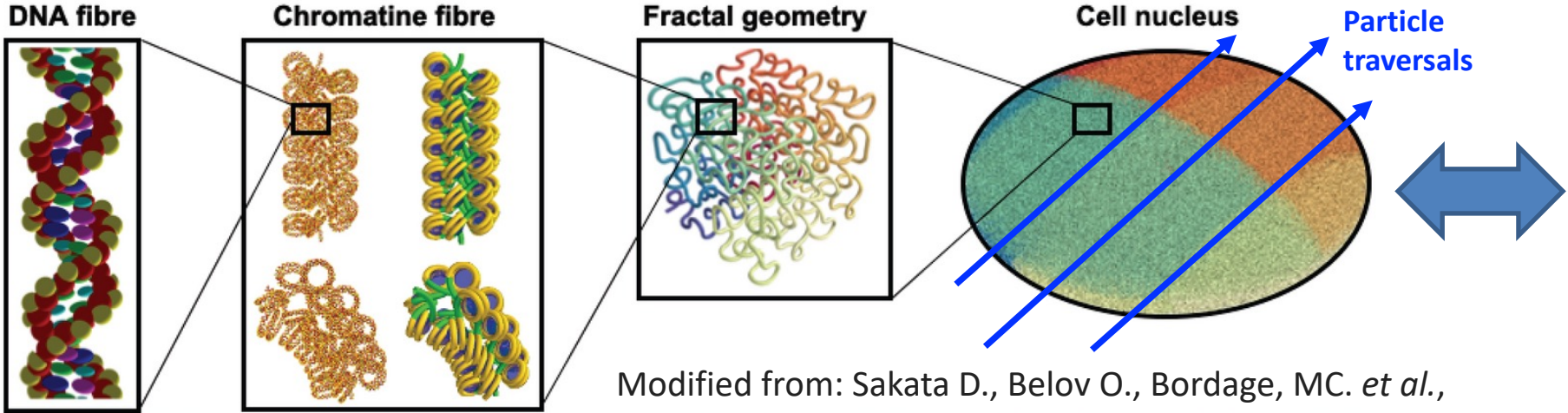
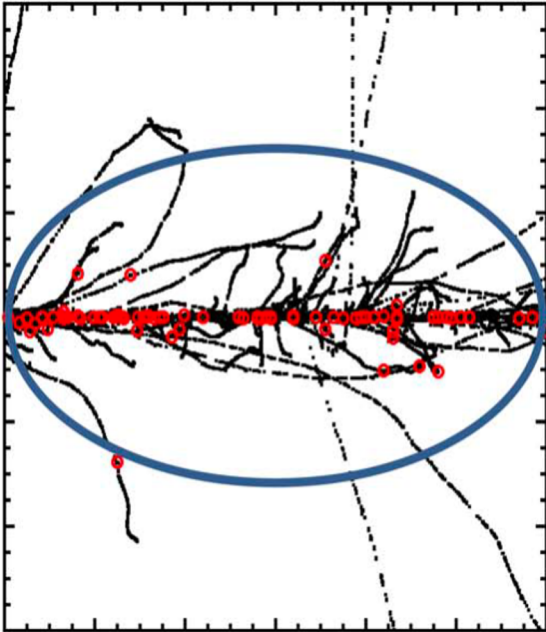
When a small sensitive target (i.e. cell nucleus) is exposed to heavy ions, the morphologically complicate structure is combined with a complicate pattern of energy deposition.

The best-known example is radiation damage to DNA.

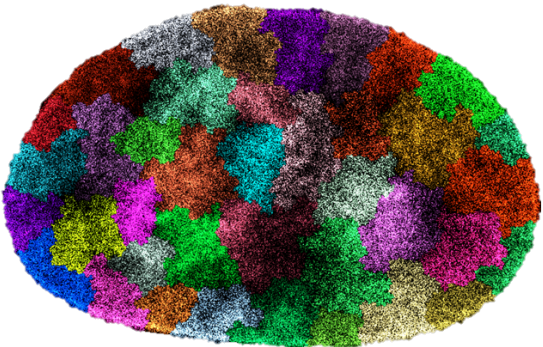
Cell nucleus has a complicate morphology structure. Each chromosome occupies the exact territory.

DNA is very tightly folded, it is compacted in a way that allows it to easily become available to the many enzymes

416 MeV/n Fe ion track + DSB



Modified from: Sakata D., Belov O., Bordage, MC. *et al.*, *Sci Rep* **10**, 20788, 2020

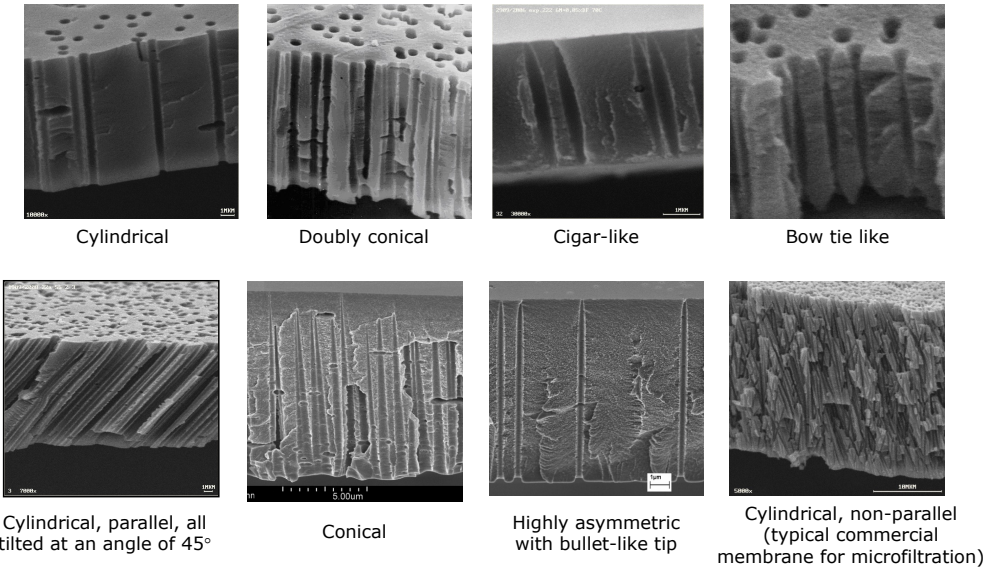


Chromosome territories (nucleus). Measurements by Kirti Prakash (Rowitch lab)

Pattern of energy deposition exhibited by heavy ions determines their practical benefits

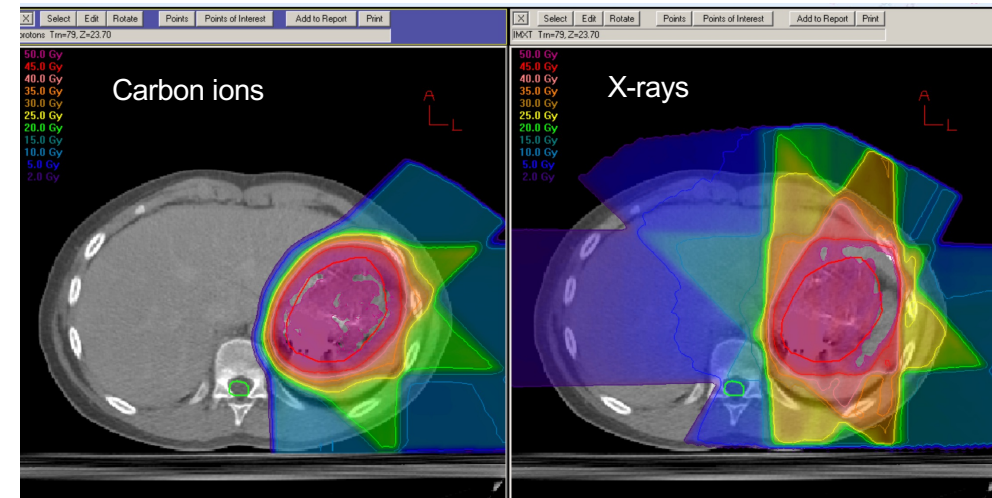
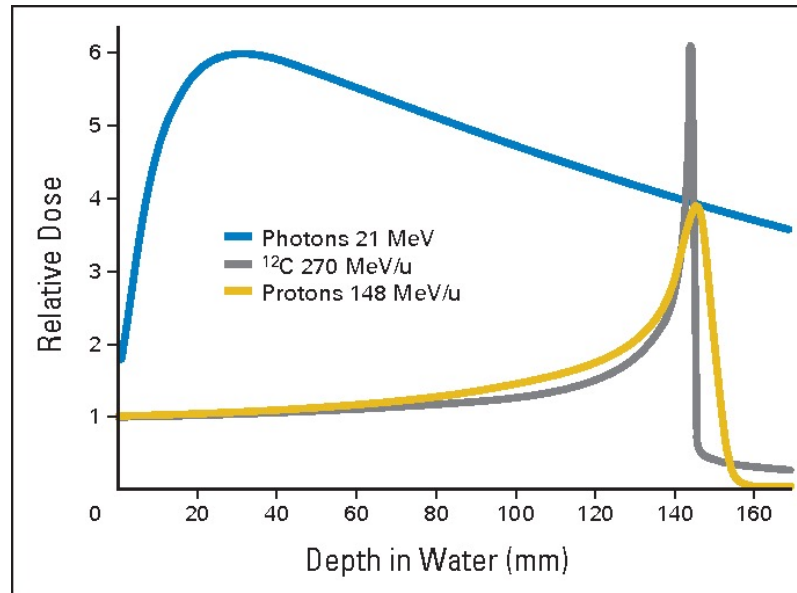
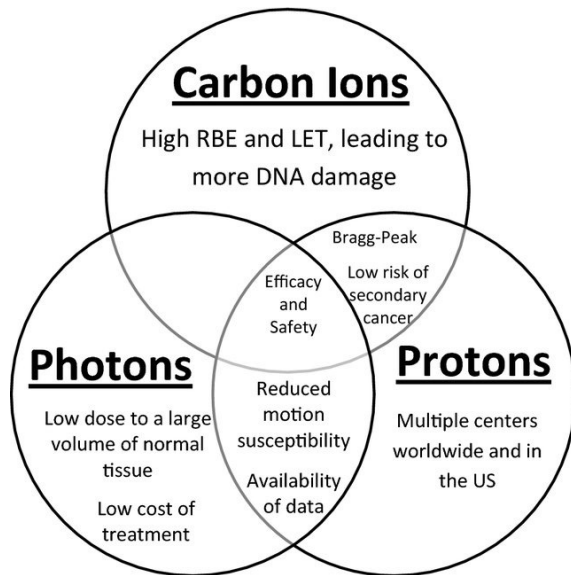
- In radiation modification of materials: there is an option to induce precise radiation defects (latent tracks), which then can be transformed into the pores with different parameters.
- In radiation medicine, ion therapy demonstrates a more precise shape around the solid tumors than sparsely ionizing radiation and even more precise than proton therapy.

Variety of pore shapes in track-etched membranes



D. Schulz-Ertner, H. Tsujii, J.Clin. Oncol. 2007

P. Apel. 2021. Applied Research @ NICA meeting



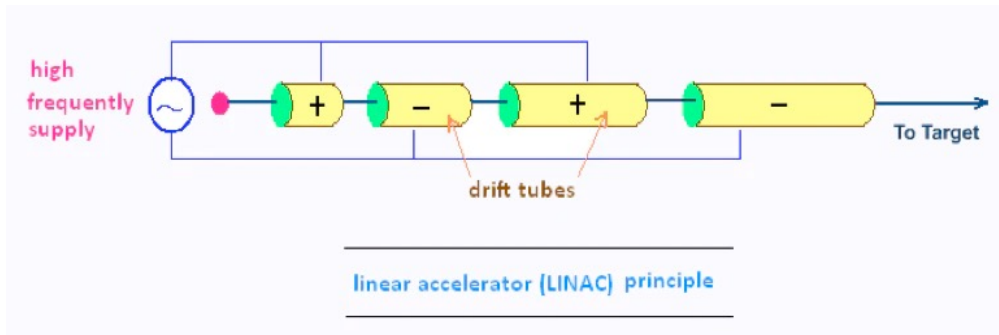
Jiade J. Lu et al. IAEA Scientific Forum, 2017

PARTICLE ACCELERATORS AS SOURCES OF HEAVY ION BEAMS

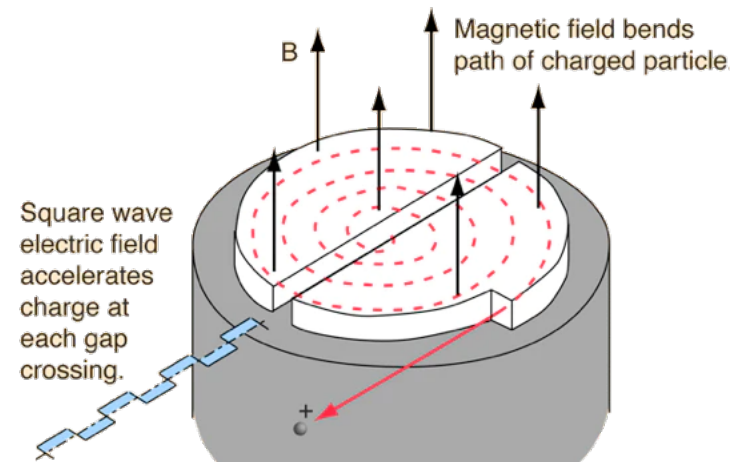
The application of the ion beams has shown great progress in the past 20 years.

Ion beam accelerators have been constructed one after another for the study of physics and fundamental sciences in the 20th century, and medical applications of ion beams advanced circa the 1980s. In the 1990s, several accelerator facilities **were established not only for fundamental science but also for biomedical and materials science study.**

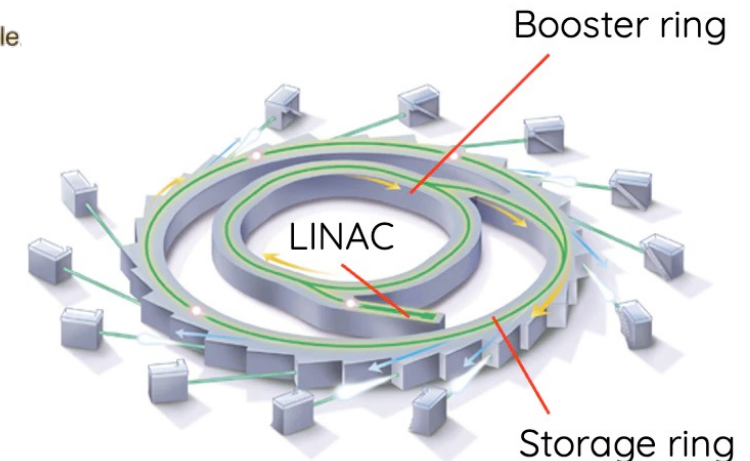
Linear Accelerators (LINAC)



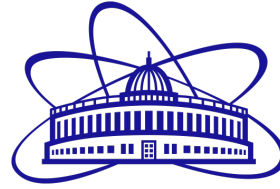
Cyclotrons



Synchrotrons



JINR FACILITIES CAPABLE OF PRODUCING HEAVY ION BEAMS



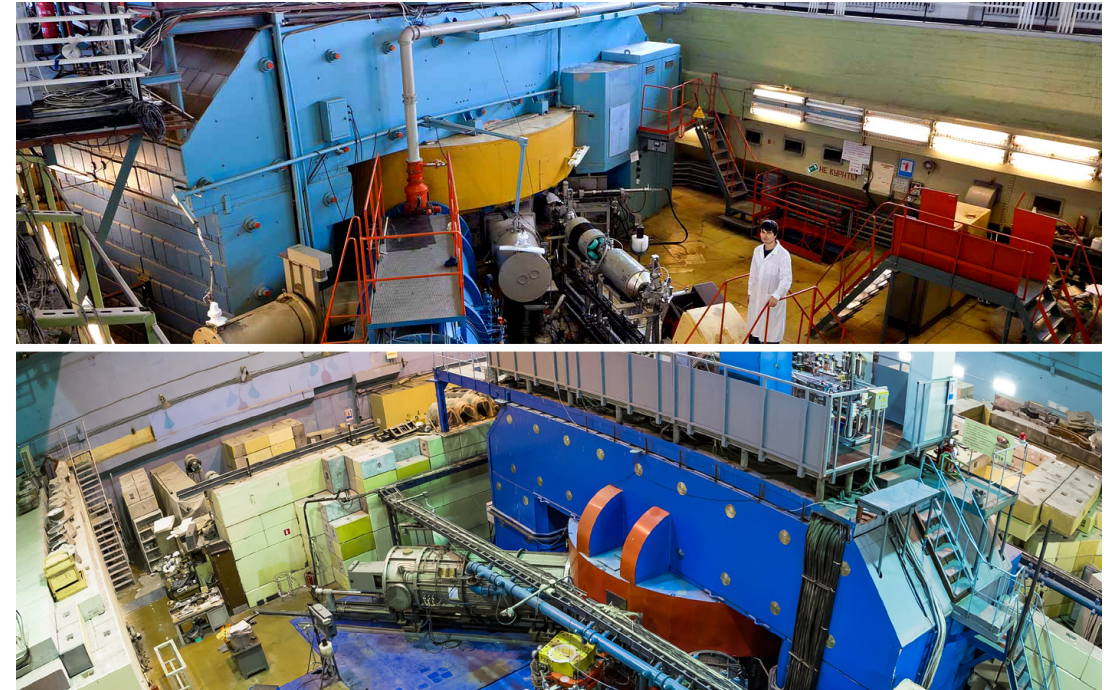
JINR

NICA accelerator complex



LINAC, HILAC, Booster, Nuclotron and Collider ring

DRIBs accelerator complex



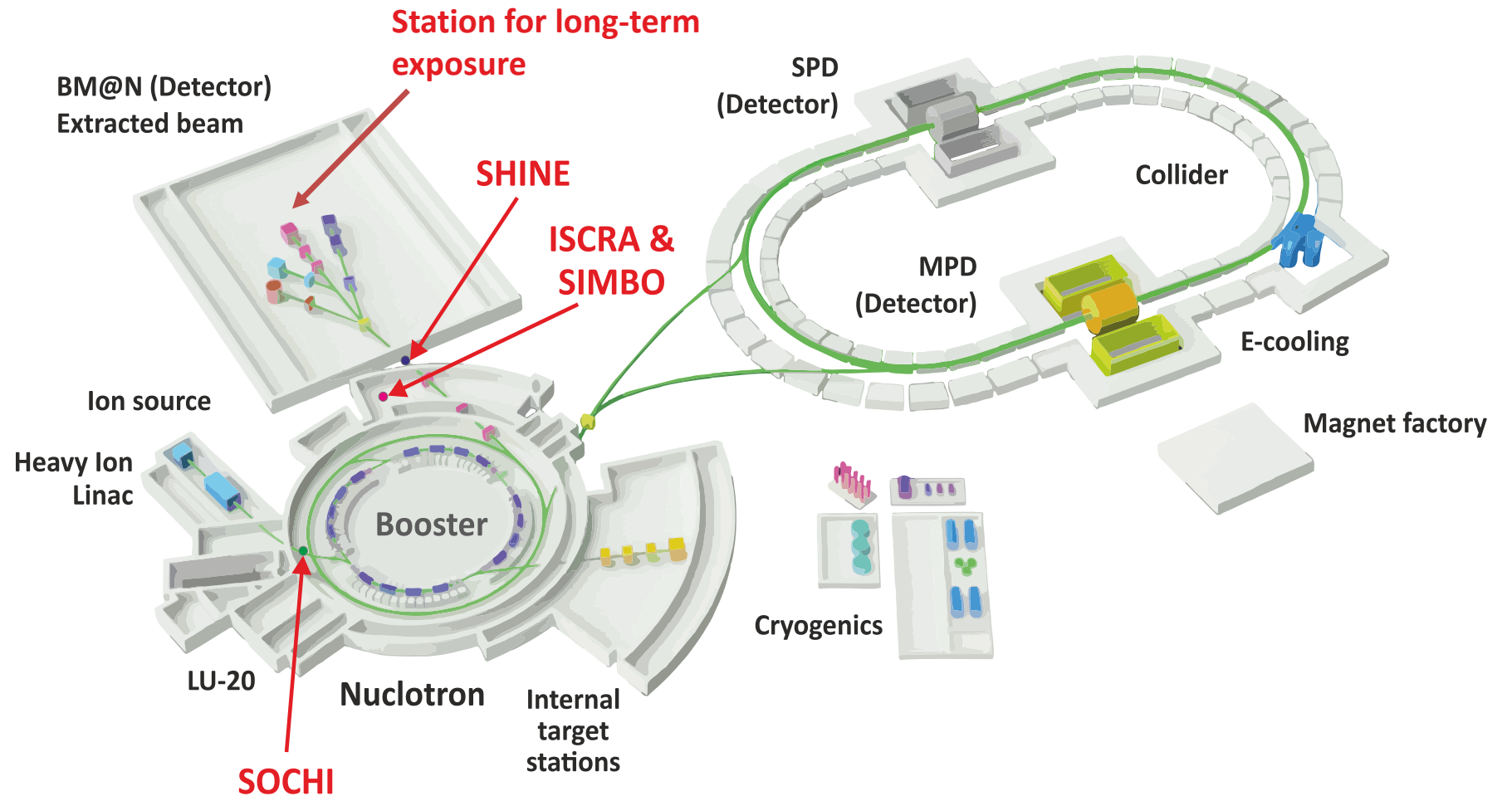
U400, U400-M and DC-280 cyclotrons

II. Applied research with NICA heavy ion beams



NICA FACILITIES FOR APPLIED RESEARCH

The **Applied Research Infrastructure for Advanced Developments at NICA facility (ARIADNA)**





APPLIED RESEARCH @ NICA



The **Applied Research Infrastructure for Advanced Developments at NICA facility (ARIADNA)** will include:

- (1) Beamlines with magnetic optics, power supplies, beam diagnostics systems, cooling systems, etc.
- (2) Experimental zones equipped with target stations for users (detectors, sample holders, irradiation control and monitoring system, etc.)
- (3) Supporting user infrastructure (areas for deployment of user's equipment, for sample preparation and post-irradiation express analyses, etc.)

Low-energy ion beams
available at HILAC
3.2 MeV/nucleon

Intermediate-energy ion beams
available at Nuclotron
150-1000 MeV/nucleon

High-energy ion beams
available at Nuclotron
up to 4.5 GeV/nucleon

Life sciences, Radiation damage to microelectronics, Materials science, Novel relativistic nuclear technology

Protons and ions with $Z = 2$ to 92

Irradiation of decapsulated microcircuits and solid materials with 3.2 MeV/nucleon ions.

Ions: $^{12}\text{C}^{6+}$, $^{40}\text{Ar}^{18+}$, $^{56}\text{Fe}^{26+}$, $^{84}\text{Kr}^{36+}$, $^{131}\text{Xe}^{54+}$, $^{197}\text{Au}^{79+}$

Irradiation of capsulated microcircuits with 150-350 MeV/nucleon ions. Ions like $^{197}\text{Au}^{79+}$ are decelerated in the capsule to 5-10 MeV/nucleon.

500-1000 MeV/nucleon ions be available at the target station for biological sample irradiation.

Ions: $^1\text{H}^{1+}$, $^2\text{D}^{1+}$, $^{12}\text{C}^{6+}$, $^{40}\text{Ar}^{18+}$, $^7\text{Li}^{3+}$

Target station will be equipped with targets from C to Pb and with the systems of beam and target diagnostics, positioning, thermometry, synchronization, radiation control, and data acquisition.

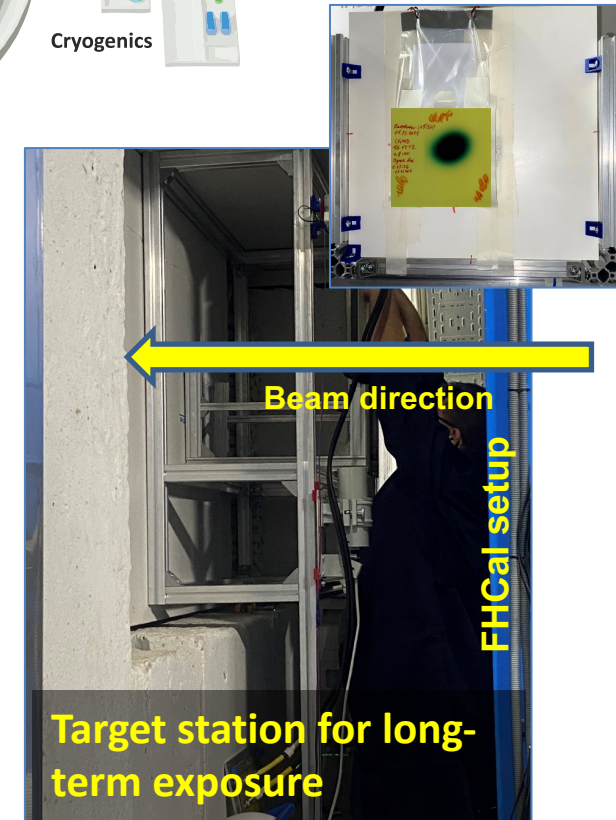
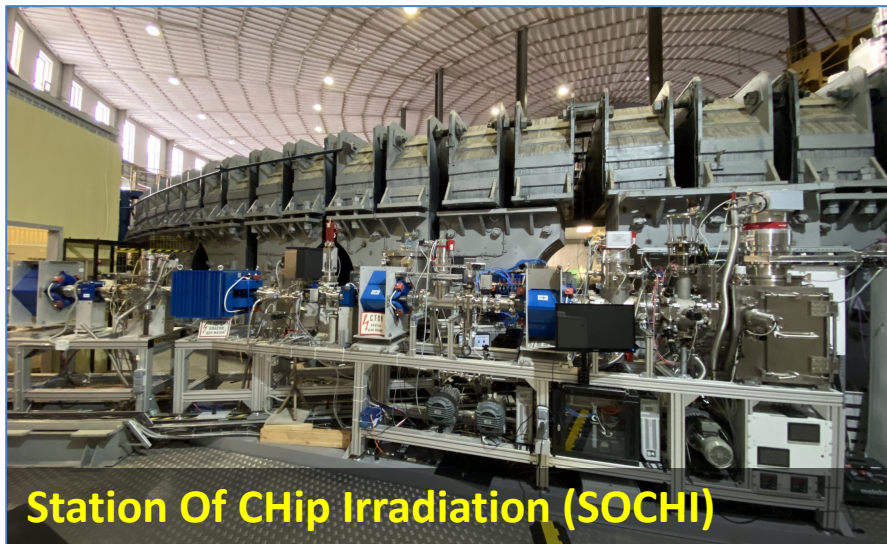
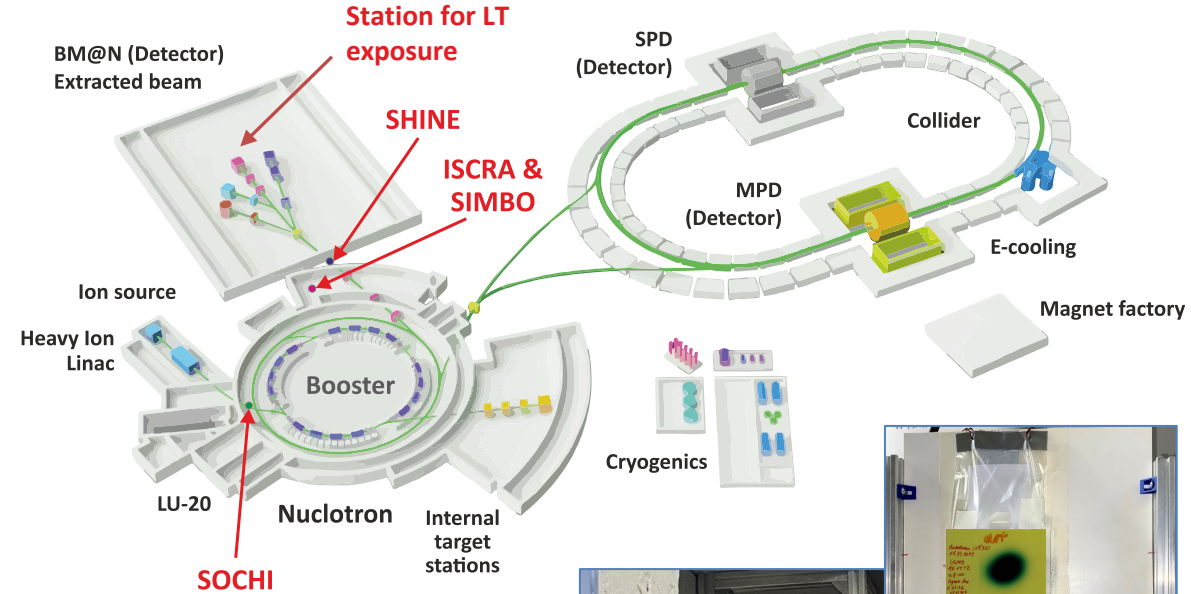
ARIADNA RESEARCH INFRASTRUCTURE: CURRENT STATE AND RECENT DEVELOPMENTS



In December 2021, the beamline and **Station Of CHip Irradiation (SOCHI)** was completed.

In December 2022, the **prototype of the Target station for long-term exposure with high energy ions** was assembled at the outgoing beam available behind the BM@N facility. This target station has an advantage to use beams for applied research purposes in parallel with operation of the BM@N setup.

In February 2024, the infrastructure of **SIMBO** and **ISCRA** beamline zone was completed.

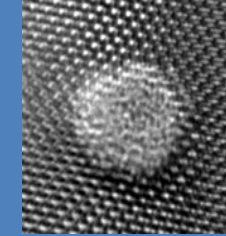
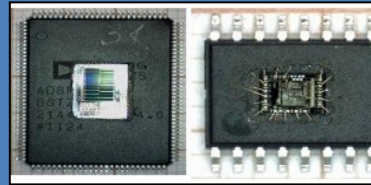


III. Sample activities and selected results

PILLARS OF APPLIED RESEARCH WITH NICA BEAMS

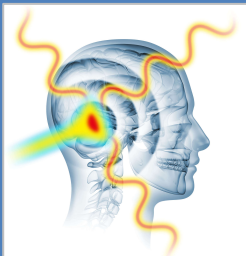
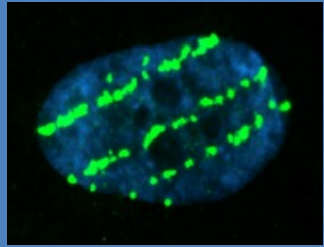
Radiation effects in microelectronics

Radiation protection on Earth and in space



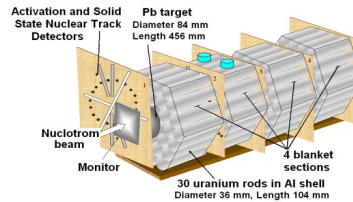
Materials research with ion beams

Radiation biophysics and radiobiology

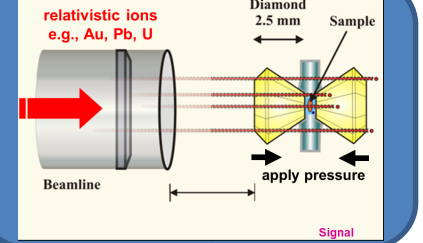


Radiation therapy-related research

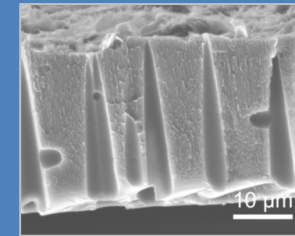
NICA



Novel technologies for accelerator-driven systems (ADS)



Materials in extreme radiation dose conditions

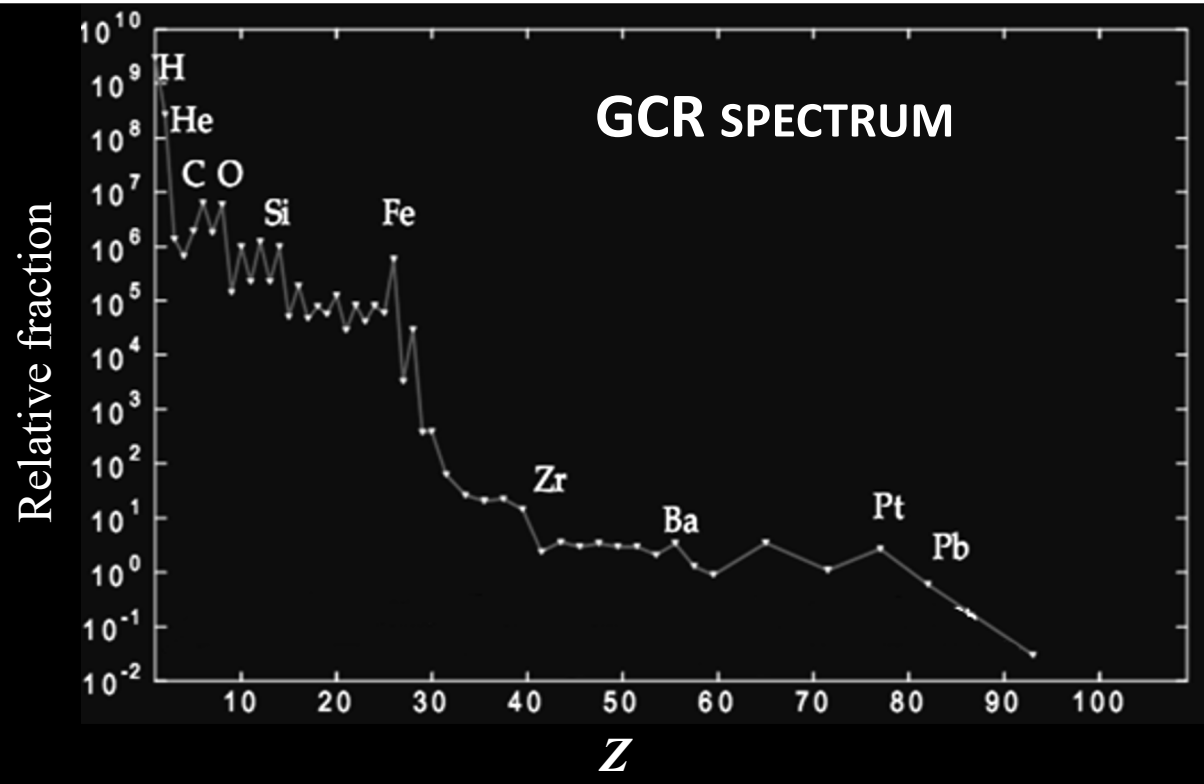


SIMULATION OF SPACE RADIATION COMPONENTS: GALACTIC COSMIC RAYS

Space radiation environment has 2 sources/types

- Galactic Cosmic Rays (GCR) have atomic # $1 \leq Z \leq 92$ and energies ~ 100 s of MeV/nucleon and higher (shielding ineffective)
- Solar Particle Events (SPE) have # $1 \leq Z \leq \sim 26$ and energies up to ~ 10 s of MeV/nucleon (shielding can be effective)

Charge

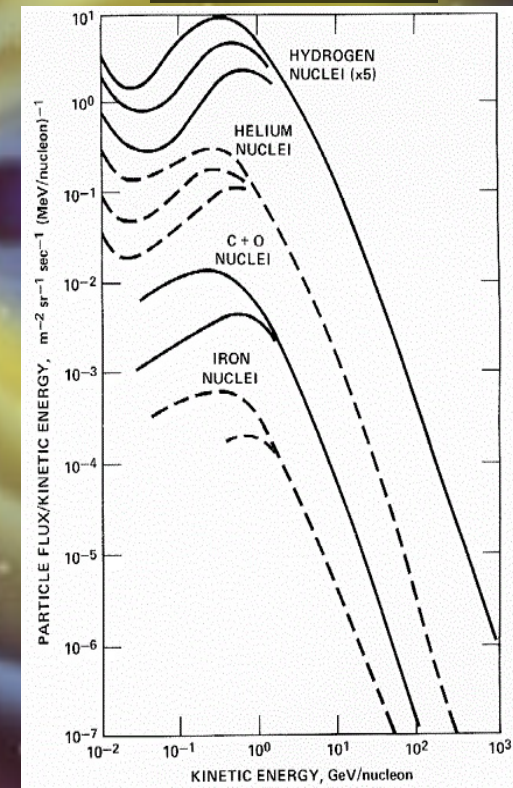


Protons ($Z = 1$) $\sim 92\%$
He ions ($Z = 2$) $\sim 7\%$
Ions with $c Z = 3 \div 5 \sim 0.1 \div 0.15\%$
Ions of $Z = 6 \div 9 \sim 0.5\%$
Ions of $Z = 10 \div 15$
Ions of $Z = 16 \div 26 \sim 0.065\%$
Fe ions ($Z = 26$) $\sim 0.025\%$

Wide range of energies
up to 10^{20} eV

/Dorman, 1975;
Kalmykov et al., 2007/

Energy

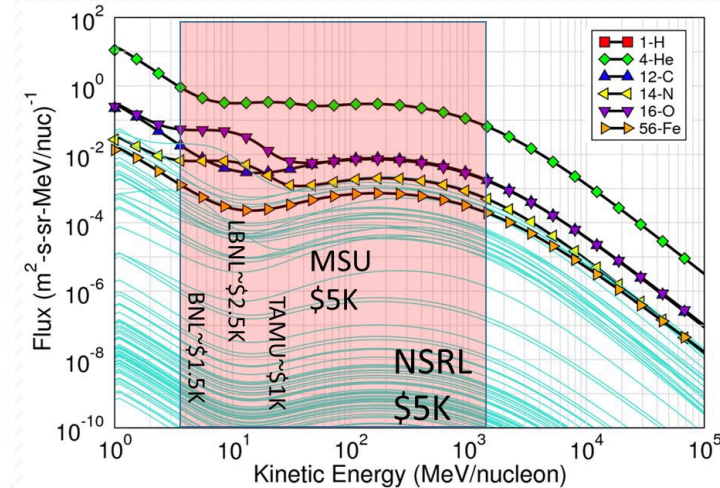
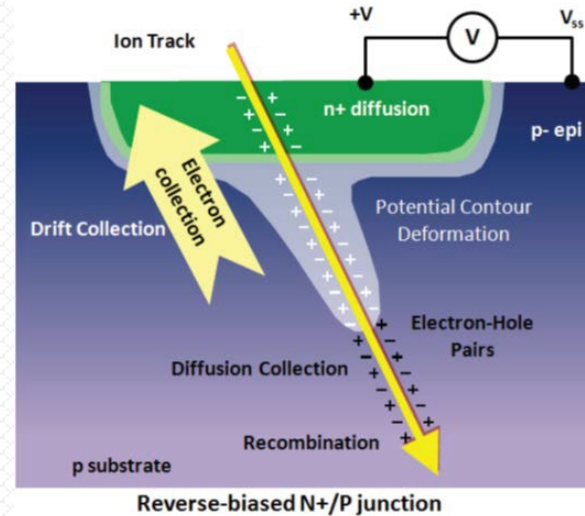


RADIATION TESTING OF ELECTRONICS WITH IONS OF RELATIVELY HIGH ENERGY

Two types of radiation effects

- Cumulative (dose) effects result from long-term exposure to radiation environment
- Single-Event Effects (SEE) occur promptly due to a single particle strike

Recent studies: 25-50% of spacecraft anomalies due to SEE (depends on spacecraft orbits)



/R.C. Baumann, 2013 NSREC Short Course/

Increasing integration poses problems for SEE testing with low-energy beams

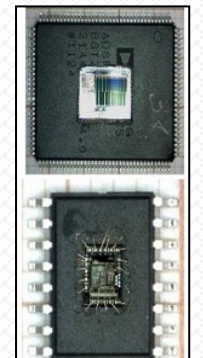
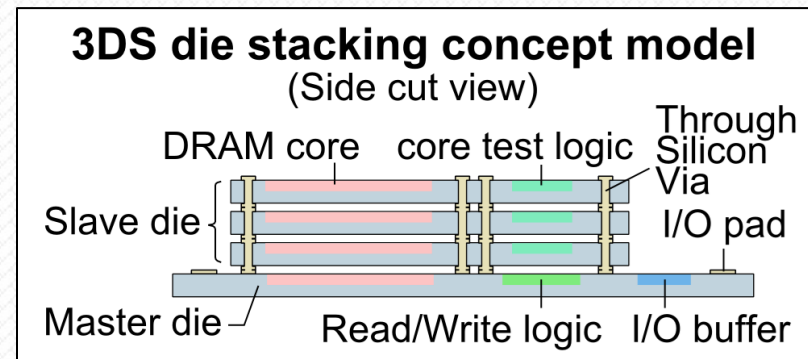
- Multiple die stacked together in packages.
- Behavior may differ if dis-assembled, tested separately.
- Packages now intrinsic to part performance.
- Dis-assembly may compromise timing, thermal and structural characteristics—especially if thinning required.

SEE Frontiers:

1. Technology Frontier
2. Low-Energy Frontier

3. High-Energy Frontier – relevant to facilities like NICA

- Ideally, prefer test with ions' characteristic relevant to space
- GCR ions fairly flat out to >2 GeV/nucleon (min. ionizing)
- Difficult and expensive to achieve at accelerators



/By R.L. Ladbury at the Meeting of the American Physical Society, Columbus, OH, April 14-17, 2018/

SAMPLE ACTIVITIES OF THE LIFE SCIENCES WORKING PACKAGE

- Molecular biology research (DNA damage and repair)
- Radiation genetics (gene and structural mutations)
- DNA repair protein biomarkers
- Aspects of the radiation-induced cell death (apoptosis, necrosis)
- Formation of chromosomal aberrations
- Different aspects of radiation-induced cancerogenesis
- Central nervous system disorders following the radiation exposure
- Development of radiation protection measures
- Improvement of beam delivery and dosimetry methods for radiotherapy
- ...

STUDY OF BEHAVIORAL AND NEUROCHEMICAL OUTCOMES IN LABORATORY ANIMALS FOLLOWING APPLICATION OF CHEMICAL AND/OR RADIATION FACTORS

(Both for space-related research and for or preclinical studies using animals to investigate the potential of a therapeutic drug or strategy)

Probing the variety of behavioral reactions in laboratory animals following application of chemical and/or radiation factors:

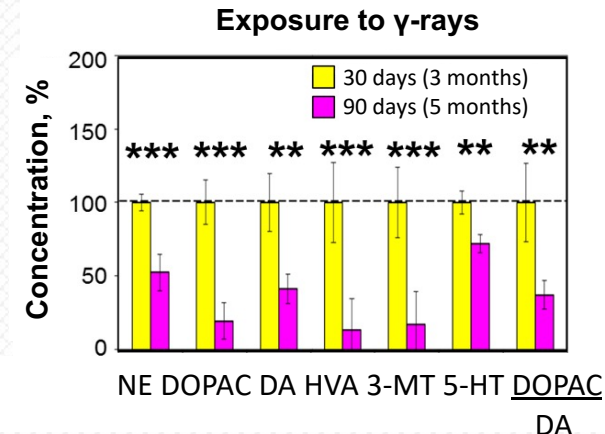
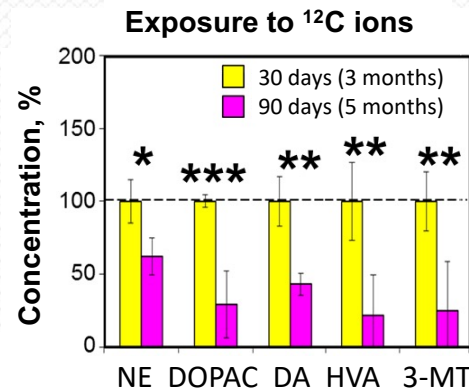
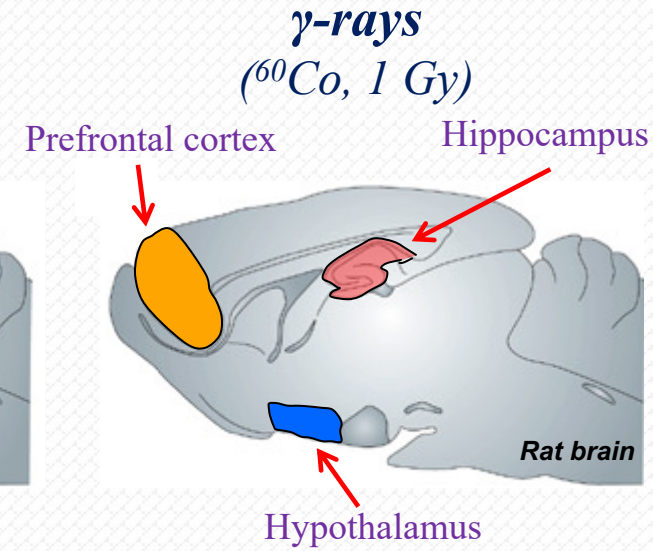
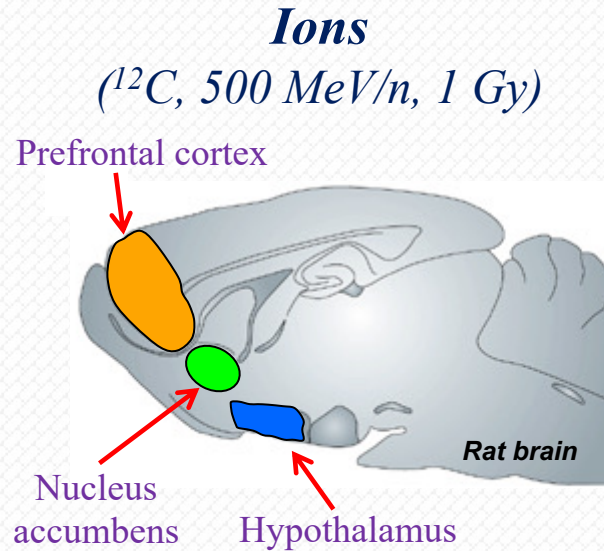
- anxiolytic-/anxiogenic-like effects;
- sedative effects;
- depression model;
- locomotor activity;
- memory;
- stress-vulnerability, etc.

Application of behavioral test sets:

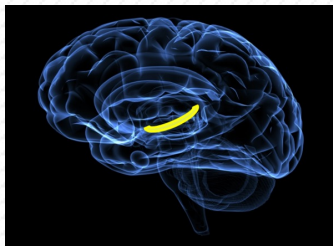
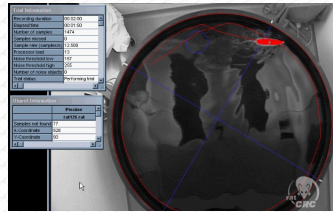
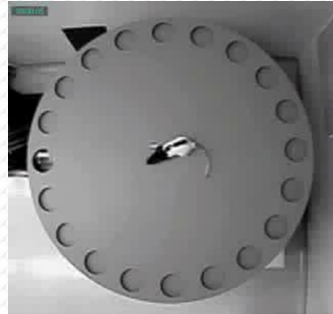
- Open Field;
- Elevated Plus Maze;
- Rotarod Performance Test;
- Passive Avoidance Task;
- etc.



Belov et al., 2015-2022



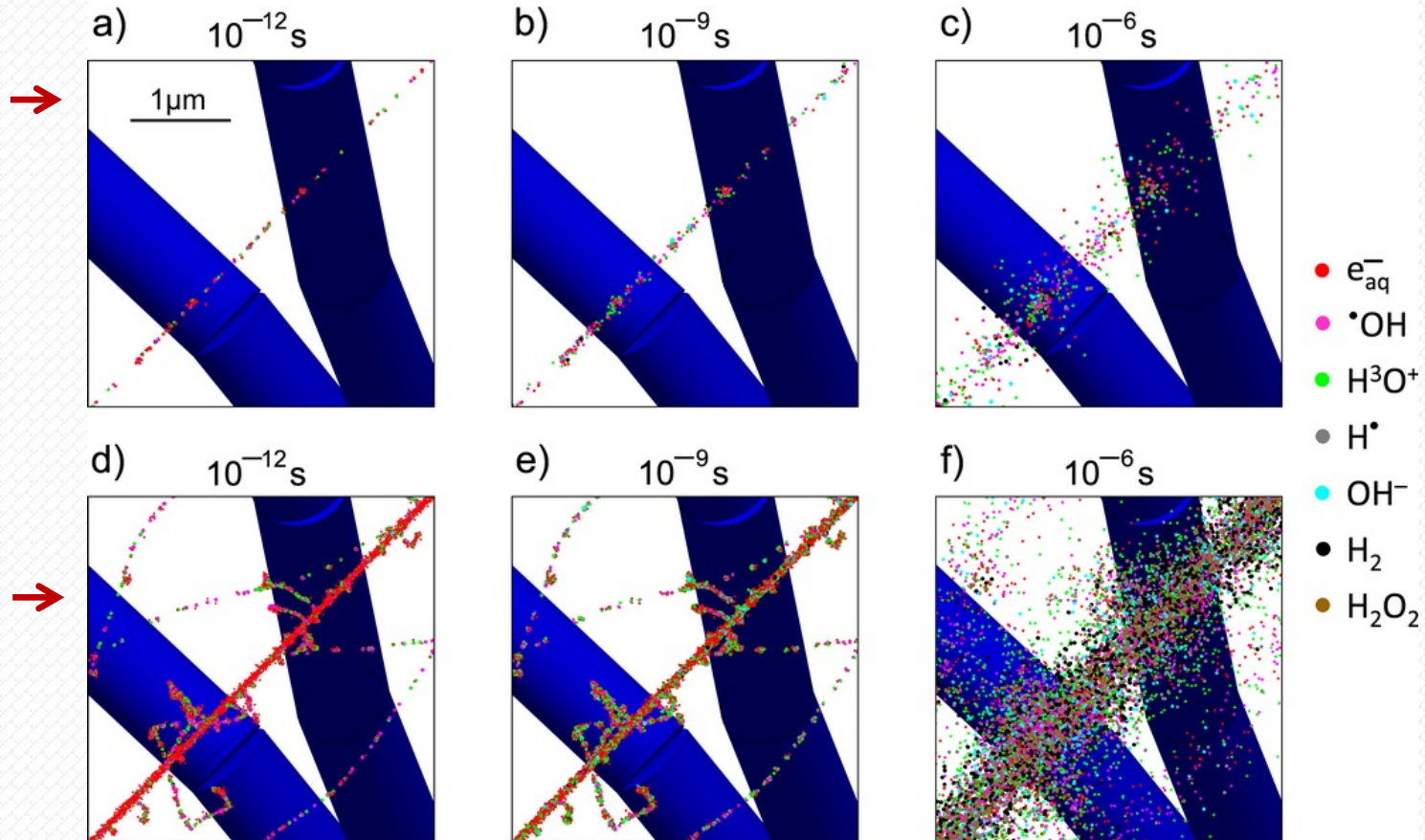
Seeking for most radiosensitive brain structures



STUDY OF RADIOLYTIC DAMAGE TO NEURAL CELL STRUCTURES

DISTRIBUTION OF FREE RADICALS IN A SINGLE PYRAMIDAL NEURON AFTER IRRADIATION

30 MeV ${}^1_0\text{p}$ particle track



1000 MeV/u ${}^{56}\text{Fe}$ particle track

Experimental verification is needed!

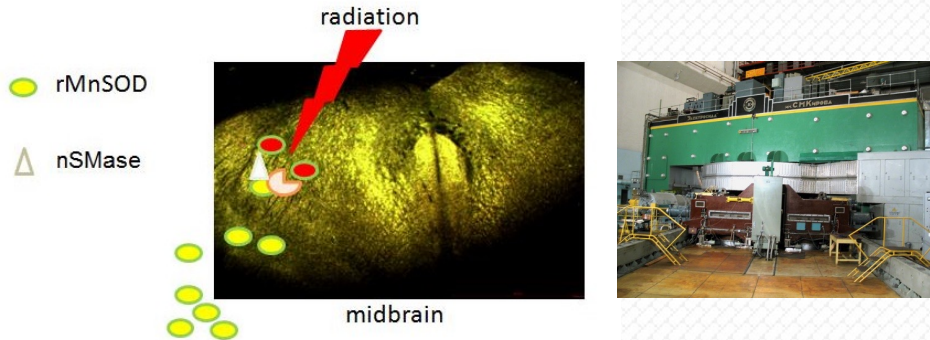
Track structure of a 30 MeV proton and 1000 MeV/u ${}^{56}\text{Fe}$ ion in dendritic branches of pyramidal neuron, as viewed at picosecond, nanosecond, and microsecond after exposure



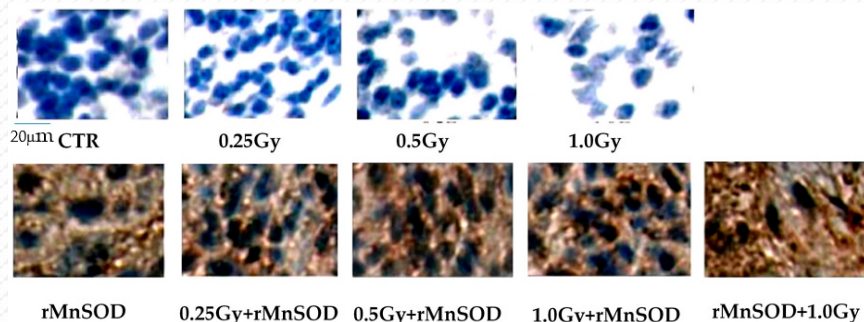
Belov et al., 2019-2021

RADIATION SAFETY AND RADIATION PROTECTION FRONTIERS: BIOMEDICAL MEASURES

Development and testing of pharmaceuticals for protecting astronauts from space radiation on experimental models of laboratory animals



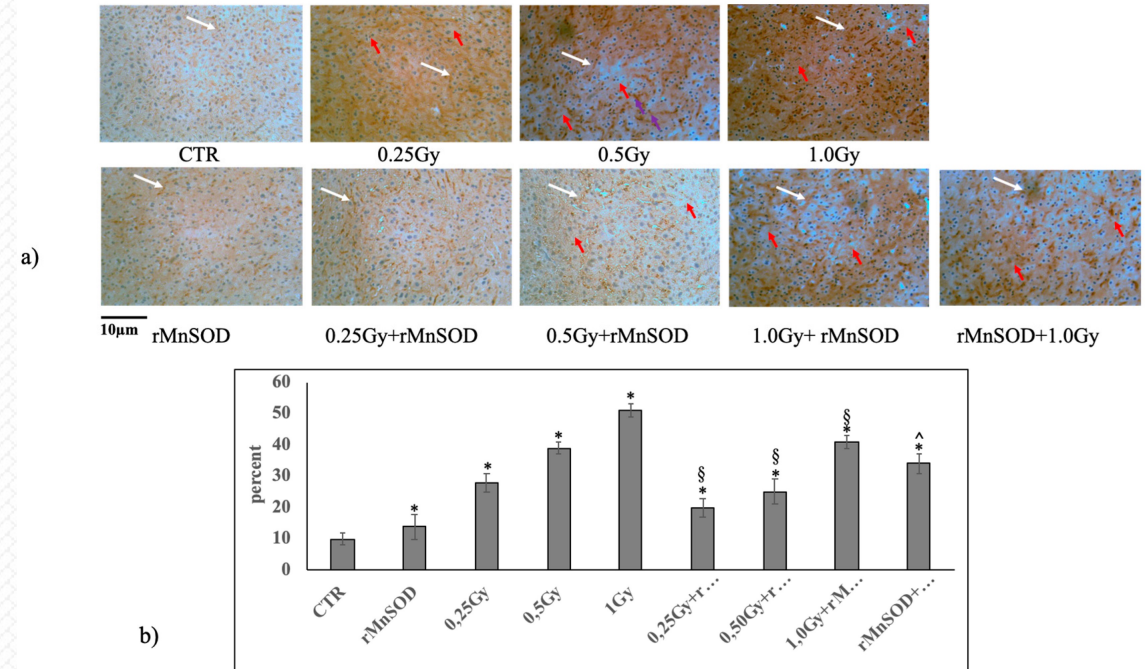
It has been established that recombinant human manganese-containing superoxide dismutase (rMnSOD), which has specific antioxidant and antiradical activity, is able to overcome the blood-brain barrier and penetrate into the midbrain, preventing radiation damage.



Localization of rMnSOD in brain tissue. Immunohistochemical analysis was performed by using specific antibody. The immunostaining was evident only in brain samples from rMnSOD-treated mice.

Cataldi, S.; Borrelli, A.; Ceccarini, M.R.; Nakashidze, I.; Codini, M.; Belov, O.; Ivanov, A., et al. Neutral Sphingomyelinase Modulation in the Protective/Preventive Role of rMnSOD from Radiation-Induced Damage in the Brain. *Int. J. Mol. Sci.* 2019, 20, 5431.

The ability of rMnSOD to reduce radiation-induced damage has been shown, both through a protective role associated with sphingomyelinase with an acidic pH optimum (aSMase), and through a prophylactic role through sphingomyelinase with a neutral pH optimum (nSMase).



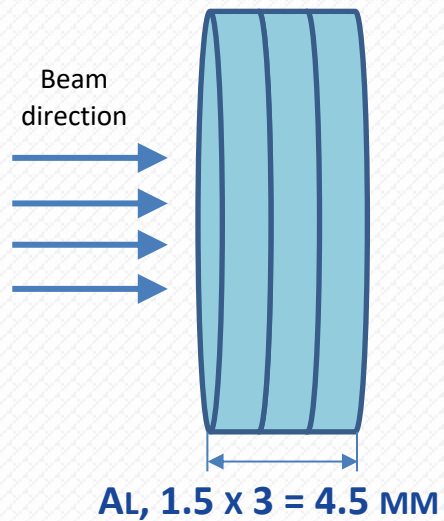
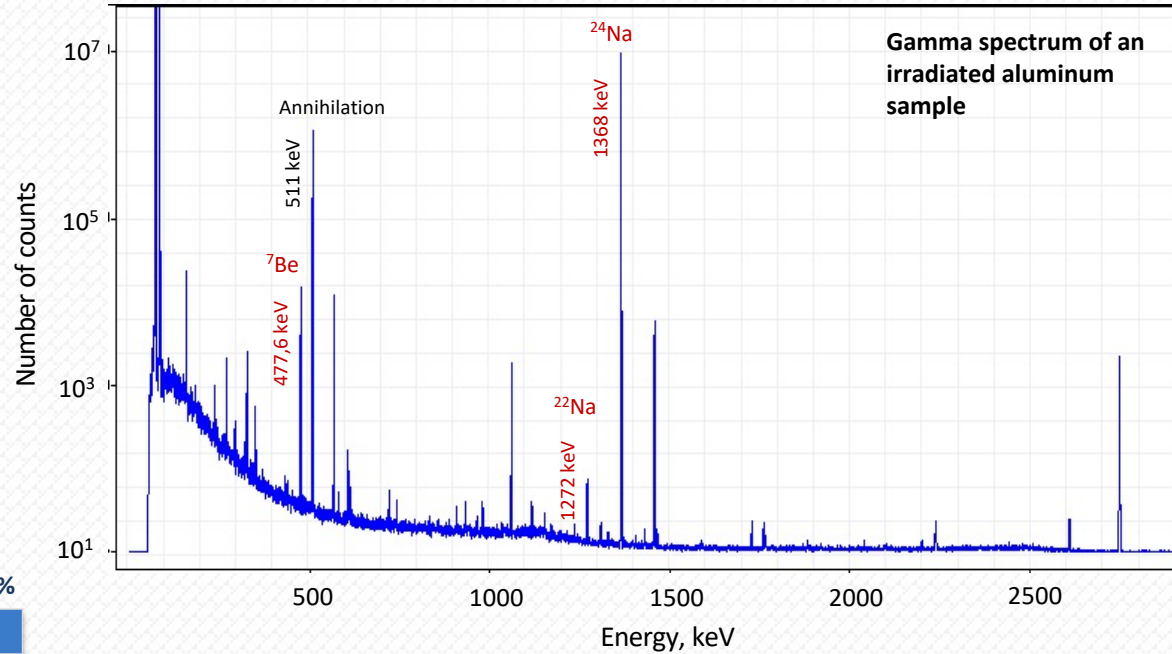
Mouse liver after irradiation with or without protective or preventive rMnSOD treatment (a) representative liver histology by Caspase-1 immunohistochemical staining. (b) Quantification of Caspase-1 staining was performed using the ImageFocus software. Positive staining is indicated as low (+), medium (++), or high (+++). Only high positive staining was considered and was measured as a percentage of the total area. Data represent the mean + S.D. of three livers for each group. Significance, * $p < 0.05$ with respect to the CTR, $^{\$} p < 0.05$ with respect to the irradiated samples, $^{\wedge} p < 0.05$ with respect to 1.0 Gy + rMnSOD.

Cataldi S, Borrelli A, Ceccarini MR, Nakashidze I, Codini M, Belov O, Ivanov A, et al. Acid and Neutral Sphingomyelinase Behavior in Radiation-Induced Liver Pyroptosis and in the Protective/Preventive Role of rMnSOD. *Int J Mol Sci.* 2020, 21(9), 3281.

ACTIVATION ANALYSIS OF MATERIALS UPON IRRADIATION WITH $^{124}\text{Xe}^{54+}$ IONS OF 3.8 GEV/NUCLEON



ALUMINUM TARGET
AMЦ 27817 (1.5 x Ø70 MM)



Composition (GOST), %

Al	96.35 — 99
Mn	1 — 1.5
Cu	0.05 — 0.2
Fe	Up to 0.7
Si	Up to 0.6
Zn	Up to 0.1



IV. Ways to be involved in the ARIADNA collaboration on applied research at NICA

ARIADNA COLLABORATIONS FOR APPLIED RESEARCH AT NICA

ARIADNA-LS Collaboration	ARIADNA-MSTE Collaboration	ARIADNA-NPT Collaboration
<p>The Collaboration is being established in order to perform experiments in the field of life sciences at the NICA Complex with the ARIADNA beamlines</p>	<p>The Collaboration is being established in order to perform activities and experiments in radiation materials science and radiation testing of electronics at the NICA Complex with the ARIADNA beamlines</p>	<p>The Collaboration is being established in order to facilitate novel developments for nuclear technology at the NICA Complex with the ARIADNA beamlines</p>

Collaborating organizations

1. Joint Institute for Nuclear Research (Dubna, Int.)
2. Institute of Biomedical Problems, RAS (Moscow, Russia)
3. Burnasyan Federal Medical Biophysical Center of Federal Medical Biological Agency (Moscow, Russia)
4. Skobeltsyn Research Institute of Nuclear Physics, Moscow State University (Dubna, Russia)
5. Saint Petersburg State University (Saint Petersburg, Russia)
6. Tsyb Medical Radiological Research Centre (Obninsk, Russia)
7. Semenov Research Center of Chemical Physics, RAS (Moscow, Russia)
8. Institute of Theoretical and Experimental Biophysics, RAS (Moscow, Russia)
9. Moscow Institute of Physics and Technology (Dolgoprudny, Russia)
10. Kurnakov Institute of General and Inorganic Chemistry, RAS (Moscow, Russia)
11. National Research Nuclear University MEPhI (Moscow, Russia)
12. Joint Institute of High Temperatures, RAS (Moscow, Russia)
13. North Ossetian State University (Vladikavkaz, Russia)
14. Institute of Nuclear Problems of the Belarusian State University (Minsk, Belarus)
15. LLC Research and production company "Kvant-R" (Moscow, Russia)
16. LLC "S-Innovations" (Moscow, Russia)
17. LLC "SOL-Instruments" (Minsk, Belarus)
18. IC CANDLE, Yerevan, Armenia
19. Yerevan State University, Yerevan, Armenia

157 participants

- Both **academic and industrial groups are eligible** to access the ARIADNA infrastructure.
- A corresponding **user policy at NICA is under development**, which includes regulations on equipment use, bioethics, access to beamlines and to supportive user infrastructure, etc.
- Funding opportunities can also be provided on the basis of **special-purpose grant programs** launched for NICA by external funding agencies.
- Main counterpart from ARIADNA users: **results need to be published!**





WAYS OF GETTING INVOLVED IN ARIADNA



- As a **member of ARIADNA collaboration**: get in touch with us and we will provide instructions on signing an MoU to become a member of the collaboration.
- As a **user**: just prepare and submit your proposal for consideration.
- As an **ARIADNA partner**: let us know how you think you/your research team or company can contribute to ARIADNA and we can prepare a relevant application to be discussed with NICA management.



THANK YOU FOR YOUR ATTENTION

CONTACT INFORMATION:

OLEG BELOV

VEKSLER AND BALDIN LABORATORY OF HIGH ENERGY PHYSICS, JOINT INSTITUTE FOR NUCLEAR RESEARCH, E-MAIL: OLEG.BELOV@JINR.INT